Simultaneous softening of acoustic and optical modes in cubic $PbTiO_3$

Izumi Tomeno,[1,*] Jaime A. Fernandez-Baca,[2,3] Karol J. Marty,[2] Kunihiko Oka,[4] and Yorihiko Tsunoda[5]

[1]*Faculty of Education and Human Studies, Akita University, Akita 010-8502, Japan*

[2]*Quantum Condensed Matter Division, Oak Ridge National Laboratory, Oak Ridge, Tennessee 37831-6393, USA*

[3]*Department of Physics and Astronomy, University of Tennessee-Knoxville, Knoxville, Tennessee 37996, USA*

[4]*Nanoelectronics Research Institute, National Institute of Advanced Industrial Science and Technology, Tsukuba, Ibaraki 305-8568, Japan*

[5]*Department of Applied Physics, School of Science and Engineering, Waseda University, Shinjuku, Tokyo 169-8555, Japan*

(Received 2 July 2012; revised manuscript received 21 October 2012; published 31 October 2012)

The phonon-dispersion relations for cubic $PbTiO_3$ ($T_c = 763$ K) have been determined along the [1,0,0], [1,1,0], and [1,1,1] directions at $T = 793$ K using inelastic neutron scattering. A set of the transverse optical (TO) branches drops sharply toward the zone center. The TO phonon curves for cubic $PbTiO_3$ are nearly isotropic, in contrast to the distinct q dependence of the TO branches for tetragonal $PbTiO_3$. The zone-center TO mode energy softens with decreasing temperature from 1173 to 793 K. Moreover, the transverse acoustic (TA) branch along $[\xi,\xi,\xi]$ shows significant softening around $\xi = 0.25$ and 0.5. The anomaly around the midpoint suggests a tendency toward forming a fourfold periodicity along the [1,1,1] direction, whereas the anomaly toward the R point results from the softening of the oxygen octahedron rotation. These two anomalies persist up to 1173 K and are weakly temperature dependent. The TA branches along [1,0,0] and [1,1,0] soften in the entire q range as the temperature approaches T_c. Although the phonon softening occurs simultaneously, the softening of the zone-center TO mode plays an important role in the single phase transition. The phonon dispersion relations for $PbTiO_3$ are discussed in connection with the simple perovskite oxides and the Pb-based relaxors.

DOI: 10.1103/PhysRevB.86.134306 PACS number(s): 63.20.−e, 77.80.−e, 77.84.−s

I. INTRODUCTION

Lead titanate $PbTiO_3$ and $BaTiO_3$ are widely recognized as important ferroelectric materials in the family of perovskite oxides ABO_3. Lead titanate $PbTiO_3$ undergoes a single first-order transition at a Curie temperature $T_c = 763$ K from a cubic paraelectric to a tetragonal ferroelectric phase. The tetragonal phase in $PbTiO_3$ remains stable down to 12 K.[1] In contrast, $BaTiO_3$ undergoes three phase transitions from a cubic to a tetragonal phase at 393 K, then to an orthorhombic phase at 278 K, and finally to a rhombohedral phase at 183 K. At room temperature, $PbTiO_3$ exhibits a high tetragonal distortion of $c/a = 1.06$,[2] whereas tetragonal $BaTiO_3$ shows a slight distortion of $c/a = 1.01$.[3] The stability of tetragonal $PbTiO_3$ has been interpreted as a consequence of the covalent nature of Pb $6s$ and O $2p$ states.[4] On the other hand, the rhombohedral ground state in $BaTiO_3$ has been attributed to the ionic character of Ba atoms.[4,5] The lattice dynamics of $PbTiO_3$ in the cubic and tetragonal phases has been investigated using inelastic neutron scattering.[6–9] In the 1970s, Shirane *et al.*[6] reported the softening of a well-defined transverse optical (TO) mode around the zone center in $PbTiO_3$, in sharp contrast with the overdamped soft mode in $BaTiO_3$.[10] They also reported that the transverse acoustic (TA) branch exhibits a dip around $\xi = 0.1$ due to the coupling with the soft TO mode. At that time, the phonon branches were only determined along the $[\xi,0,0]$ direction at 783 K ($T_c + 20$ K).[6] Recently Tomeno *et al.*[7] determined the phonon dispersion relations in tetragonal $PbTiO_3$ along high-symmetry directions. The zone-boundary acoustic phonon energies for $PbTiO_3$ are considerably lower than those for $BaTiO_3$. The broadened TO A_1 mode at the Γ point shows a gradual softening with increasing temperature up to 0.84 T_c, whereas the well-defined TO-E mode is weakly temperature dependent in the same range. All the reported room-temperature measurements[6–8] provide support for the first-principles phonon calculations for tetragonal $PbTiO_3$.[11,12] More recently, Kempa *et al.*[9] measured the phonon dispersion relations along the $[\xi,0,0]$ and $[\xi,\xi,0]$ directions for cubic $PbTiO_3$. Their results differ from the results of Shirane *et al.*[6] These authors[9] reported that the TA phonon curve along $[\xi,0,0]$ has no dip associated with the mode coupling and that the zone-center TO mode exhibits a strong but incomplete softening at 775 K ($T_c + 12$ K). Ghosez *et al.*[13] computed the full phonon dispersion relations for cubic $PbTiO_3$ and cubic $BaTiO_3$ using first-principles calculations. A variety of low-energy or unstable phonon branches is predicted for cubic $PbTiO_3$, but these theoretical predictions have not been experimentally verified.

Lead titanate $PbTiO_3$ is an end member of the Pb-based perovskite relaxors such as $(1-x)Pb(Zn_{1/3}Nb_{2/3})O_3$-$x$$PbTiO_3$ (PZN-xPT) and $(1-x)Pb(Mg_{1/3}Nb_{2/3})O_3$-$x$$PbTiO_3$ (PMN-xPT).[14–16] The prototype relaxor PZN undergoes a cubic to rhombohedral phase transition at the temperature $T_{C-R} \sim 385$ K.[17,18] In contrast, the average crystal symmetry of the other prototype relaxor PMN remains cubic down to 5 K.[19] The huge piezoelectric response is found in PZN-xPT with $x \sim 0.09$ and PMN-xPT with $x \sim 0.35$ near the morphotropic phase boundary between the rhombohedral and tetragonal phases.[20,21] In cubic $PbTiO_3$, the dielectric constant ϵ is expressed by the Curie-Weiss law $\epsilon = C/(T - T_0)$, where C is the Curie constant, and T_0 is the extrapolated Curie temperature.[22] Generally the difference between T_c and T_0 reflects the first-order character of the ferroelectric phase transition.[23] In the Pb-based relaxors, the dielectric constant ϵ exhibits a broad and frequency-dependent peak as a function of temperature.[24–26] The dielectric-peak temperature T_{max} in the relaxors shifts to higher temperatures with increasing frequency. In these relaxors, the dielectric constant ϵ shows a deviation from the Curie-Weiss law below the so-called Burns

temperature T_d.[26,27] The deviation from the Curie-Weiss law has been related to the growth of polar nanoregions below T_d. For PZN the Burns temperature T_d is approximately 750 K, much higher than the transition temperature $T_{C-R} \sim$ 385 K.[27] For PMN the Burns temperature T_d is 620 K, whereas the dielectric-peak temperature $T_{\max}$ is 276 K at 100 kHz.[27,28] The dielectric relaxation measurements suggest that the dynamics of polar nanoregions in PMN freezes at the freezing temperature $T_f \sim 220$ K.[25,29] For PZN, the freezing temperature T_f is close to the phase transition temperature $T_{C-R} \sim 385$ K.

Since Gehring, Park, and Shirane[30] found a steep drop of the TO phonon branch into the TA branch at a characteristic wave vector $q_{wf} \sim 0.13$ r.l.u. in PZN-0.08PT, phonon dispersion relations for the Pb-based relaxors have been extensively investigated.[31–41] In these relaxors, the TO mode merges into the TA mode toward the characteristic wave vector q_{wf} and then disappears in the range $q \leqslant q_{wf}$. The soft mode anomaly in the relaxors, named as the "waterfall" phenomenon,[30,32] has been the subject of intense debate.[30–40,42,43] The waterfall phenomenon in PMN was observed in the temperature range between T_f and T_d. Initially, Gehring and coauthors[30,32,33] argued that the characteristic wave vector q_{wf} in PZN, PMN, and PZN-0.08PT corresponds to the average size of polar nanoregions, $2\pi/q_{wf} \sim 30$ Å. Their explanation is based on the assumption that the TO mode in the range $q \leqslant q_{wf}$ is scattered by the inhomogeneous polarization. Subsequently, the waterfall phenomenon was closely associated with the broadening of the TA mode.[40] It was argued that the wavelength of the TA mode in PMN is comparable to the size of the polar nanoregions between T_f and T_d. On the other hand, Hlinka *et al.*[37] explained the waterfall effect in terms of the coupling between TO and TA modes. Unlike the relaxor PMN, the system PMN-0.6PT shows a well-defined phase transition from cubic to tetragonal structures at the temperature $T_{C-T} \sim$ 550 K.[39] The TO branch in cubic PMN-0.6PT exhibits the waterfall phenomenon, whereas the TO branch in tetragonal PMN-0.6PT stiffens considerably at the zone center. These observations suggest that the growth of polar nanoregions is not essential to the waterfall effect. Stock *et al.*[39] interpreted that the waterfall phenomenon observed in PMN and PMN-0.6PT is caused by random fields resulting from the intrinsic chemical disorder at the B site. For the relaxor PMN, the soft TO mode was also found on the Brillouin-zone edge between $q = (0.5,0.5,0)$ and $q = (0.5,0.5,0.5)$.[41]

Lead titanate $PbTiO_3$ is also an end member of the solid solution $PbZr_xTi_{1-x}O_3$ (PZT), which shows an enhanced piezoelectric response near the morphotropic phase boundary around $x = 0.5$.[44] The lattice dynamics of PZT was investigated by inelastic x-ray scattering.[45] On cooling, the soft mode at the zone boundary $q = (0.5,0.5,0)$ exhibits a crossover from vibrational- to relaxational-type dynamics. The lattice dynamics of cubic $PbTiO_3$ with simple perovskite structure is expected to provide a key to an understanding of the Pb-based complex perovskites PZN-xPT, PMN-xPT, and PZT.

In the present paper, we report the phonon dispersion relations for cubic $PbTiO_3$ at $T = 793$ K ($T_c + 30$ K) using inelastic neutron scattering. Softening of the TO and TA modes was observed between 793 K and 1173 K ($T_c + 410$ K). Next, our experimental results are compared with previous experimental studies for tetragonal and cubic $PbTiO_3$[6,7,9] and the first-principles calculations for cubic $PbTiO_3$.[13,46] Then, we discuss the lattice dynamics of $PbTiO_3$ in conjunction with the simple perovskites ABO_3 and the Pb-based complex perovskites.

II. EXPERIMENT

The inelastic neutron scattering experiments were performed on the triple-axis spectrometers TAS-1 and T1-1 at JRR-3M in the Japan Atomic Energy Agency, and HB-3 at the High Flux Isotope Reactor, Oak Ridge National Laboratory. Pyrolytic graphite (PG) crystals were used as monochromator and analyzer. A PG filter was used to reduce higher order wavelength contaminations. Both constant-**Q** and constant-E scans were employed. The TAS-1 and T1-1 spectrometers were operated with fixed incident energy, $E_i = 14.7$ meV. Collimation was 40′-40′-40′-40′ for TAS-1, and guide-40′-40′-40′ for T1-1. The HB-3 spectrometer was operated with fixed final energy, $E_f = 14.7$ meV. Collimation was either 48′-20′-20′-70′ or 48′-40′-40′-70′. The energy resolution for TAS-1 and T1-1 was 0.66 meV in full width at half maximum (FWHM) at zero energy transfer, whereas that for HB-3 was 0.91 or 1.07 meV.

Six single crystals of $PbTiO_3$ with masses ranging from 3.1 to 6.5 g were used in this study. These single crystals were grown from a PbO flux using the top-seeded growth technique. Details of the crystal growth have been described previously.[47] One of these crystals was attached on a nickel sample holder and then mounted in an electric furnace. The sample in the furnace was kept in air to avoid the possible loss of oxygen. Most of the measurements were performed at 793 K, but selected phonons were also determined up to 1173 K. A new crystal was used in the case that the crystal had been damaged or partly cracked after high-temperature experiments.

III. PHONON DISPERSION RELATIONS

Figure 1 shows the phonon dispersion relations along the high-symmetry directions $[\xi,0,0]$ (Δ), $[\xi,\xi,0]$ (Σ), and $[\xi,\xi,\xi]$ (Λ) in cubic $PbTiO_3$ measured at $T = 793$ K ($T_c + 30$ K). The Σ_3 branches represent the transverse phonons propagating in the $[1,1,0]$ direction with $[1,\bar{1},0]$ polarization, and the Σ_4 branches correspond to those with $[0,0,1]$ polarization. Table I presents the phonon energies at the end points of the transverse branches. Symmetry labels follow the convention of Ref. 48. Here the atomic positions in cubic $PbTiO_3$ are as follows: Pb at (0,0,0), Ti at (0.5,0.5,0.5), O_1 at (0.5,0.5,0), O_2 at (0.5,0,0.5), and O_3 at (0,0.5,0.5). The zone-boundary mode assignments are made for the cubic phase, on the basis of the comparison between experimental and theoretical results for cubic and tetragonal $PbTiO_3$.[7,11,13]

The phonon dispersion curves for cubic $PbTiO_3$ are compared in Fig. 2 with those for tetragonal $PbTiO_3$ at 295 K.[7] For tetragonal $PbTiO_3$, the labeling of the end points of phonon branches follows the same notation as used in Refs. 7 and 11.

These experiments clearly show the simultaneous softening of the transverse phonons at the structural phase transition in $PbTiO_3$. There are four types of soft modes in cubic $PbTiO_3$

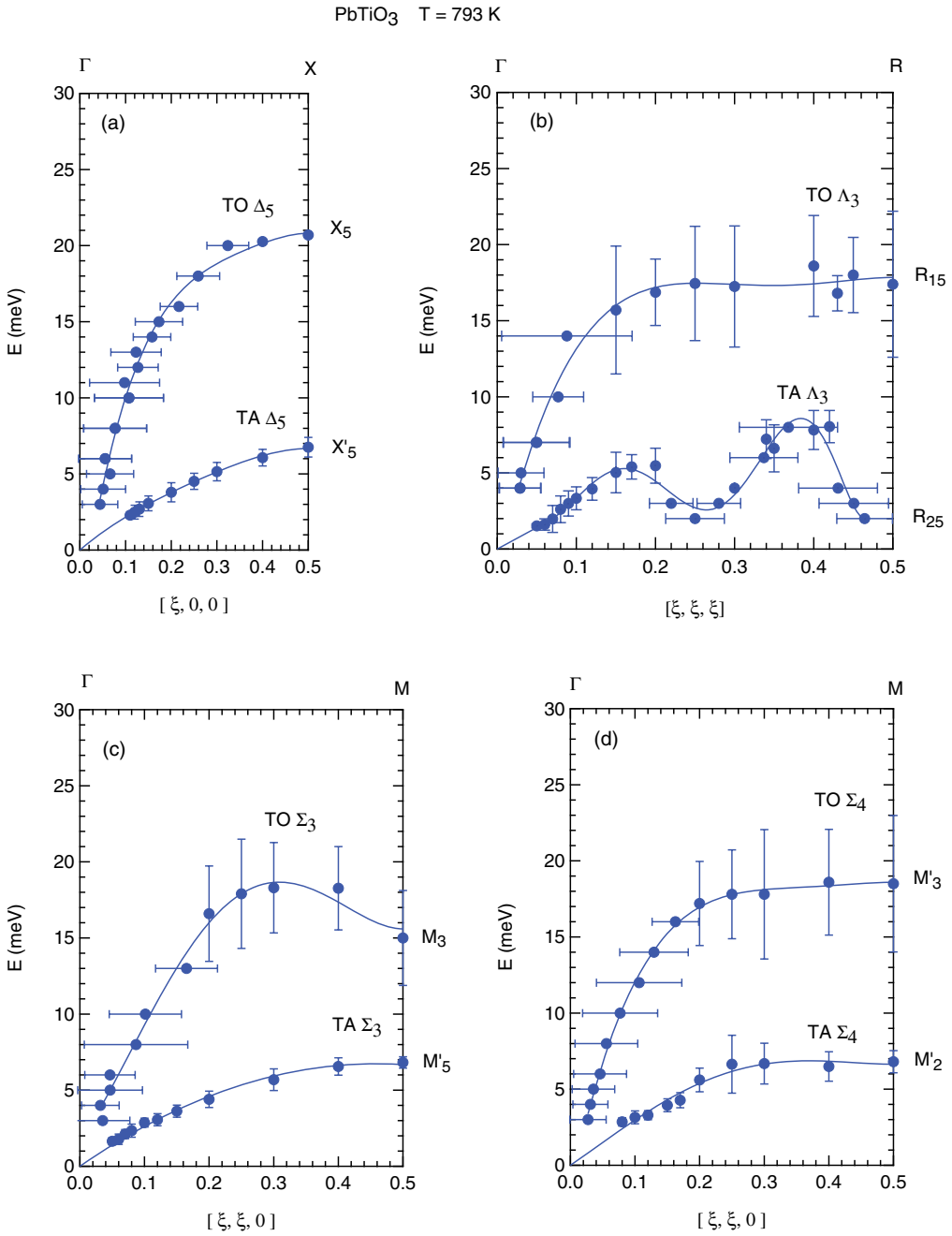

FIG. 1. (Color online) Phonon dispersion curves for cubic $PbTiO_3$ measured at $T = 793$ K ($T_c + 30$ K). Each solid circle and the attached bar refer to the phonon peak and its FWHM, respectively. Solid lines are guides to the eye.

as follows: (1) the TO Δ_5, Σ_3, Σ_4, and Λ_3 modes toward the Γ point (0,0,0), (2) the TA Λ_3 mode toward the R point (0.5,0.5,0.5), (3) the TA Λ_3 mode around the midpoint (0.25,0.25,0.25), and (4) the TA Δ_5, Σ_3, and Σ_4 branches in the entire q range.

A. TO modes

1. Zone-center TO mode

The phonon dispersion curves of the TO Δ_5, Σ_3, Σ_4, and Λ_3 modes fall sharply toward the Γ point at $T = 793$ K. A comparison of phonon branches in Fig. 3 shows that the steep dispersion of these soft TO modes toward Γ is nearly isotropic and confined to the region $\xi < 0.2$. The low-lying TO phonon at Γ is the polar Γ_{15} mode. Theoretical calculations show that the displacement of Pb atom plays an important part in the unstable Γ_{15} mode.[13,46] Figure 4 shows typical constant-E scans along the $[2-H,2+H,0]$ and $[H,H,2]$ directions at $T = 793$ K. The double-peak structure is observed around (2,2,0) and (0,0,2) down to $\Delta E = 3$ meV. Figure 4(b) shows that the scan profile at 2 meV is described by a single peak at (0,0,2). The shoulders denoted by arrows in Fig. 4(a) are due to the TA Σ_3 phonon peaks. Here the assignment to the TA mode was identified by a set of the constant-**Q** scans at

TABLE I. Phonon energies at the end points of the transverse branches in cubic $PbTiO_3$ at 793 K. Symmetry labels follow the convention of Ref. 48. The oxygen positions in reduced coordinates are taken as (0.5,0.5,0) for O_1, (0.5,0,0.5) for O_2, and (0,0.5,0.5) for O_3.

Point	Label	Normal mode	Phonon energy (meV)
TA X (0,0,0.5)	X_5'	Pb_x, O_{1x} ($x \leftrightarrow y$)	6.8 ± 0.1
TA M (0.5,0.5,0)	M_5'	Pb_x, Ti_y, O_{1y} ($x \leftrightarrow y$)	6.8 ± 0.2
TA M (0.5,0.5,0)	M_2'	Pb_z	6.8 ± 0.2
TA R (0.5,0.5,0.5)	R_{25}	$O_{2x} = -O_{3y}$	∼0 to ∼2
TO Γ (0,0,ξ), $\xi \to 0$	Γ_{15}	Pb_x, Ti_x, O_{1x}, O_{2x}, O_{3x} ($x \leftrightarrow y$)	2.5 ± 0.5
TO X (0,0,0.5)	X_5	Ti_x, O_{2x}, O_{3x} ($x \leftrightarrow y$)	20.7 ± 0.4
TO M (0.5,0.5,0)	M_3	$O_{2x} = -O_{3y}$	15.0 ± 0.3
TO M (0.5,0.5,0)	M_3'	Ti_z, O_{1z}	18.5 ± 0.3
TO R (0.5,0.5,0.5)	R_{15}	Pb_x, $O_{1y} = O_{2z}$	17.4 ± 0.3

$(2-H,2+H,0)$. A series of constant-E scans in Fig. 4 suggests that the zone-center TO phonon energy E_0 lies between 2 and 3 meV at 793 K.

The temperature dependence of zone-center TO phonon energies E_0 was determined from the constant-E scan measurements. We also performed constant-**Q** scans at (2,2,0) at several temperatures. Unfortunately, it was difficult to separate the zone-center TO mode from the tail of the strong intensity centered at $E = 0$. Figure 5 shows a series of constant-E scans along the $[2,2,L]$ direction measured at $T = 793$, 973, 1073, and 1173 K. For example, the double peak is found in Fig. 5(c) for $\Delta E = 8$ and 10 meV at 1073 K. The double-peak structure at 1073 K becomes a broad single peak for $\Delta E = 6$ meV, and then the flat background is observed for $\Delta E = 5$ meV. The sequence of the scan profiles at 1073 K reflects the presence of the TO phonon dispersion across the Γ point at $E_0 = 6$ meV. In the range $\Delta E \leqslant 4$ meV, the TA Δ_5 mode contributes to the shoulder peaks denoted by arrows in Fig. 5. The TA branches are also found to vary with temperature, as will be shown in Sec. III B.

Figure 6 shows the zone-center TO phonon energy E_0 as a function of temperature. The dielectric properties in $PbTiO_3$ above T_c are difficult to study because of the high electrical conductivity.[22,49] For slightly uranium-doped $PbTiO_3$, the dielectric constant ϵ in the paraelectric phase is given by $\epsilon = C/(T - T_0)$ with $C = 4.1 \times 10^5$ K and $T_0 = 722$ K in the range up to 873 K ($T_c + 110$ K).[22] Thus the zone-center TO phonon energy E_0 in $PbTiO_3$ is expected to have the form $E_0 = A(T - T_0)^{0.5}$ above T_c, in light of the Curie-Weiss law and the Lyddane-Sachs-Teller (LST) relation. In Fig. 6 the solid line above T_c is a least-squares fit to the data with $A = 0.36 \pm 0.02$ meV/K$^{0.5}$ and $T_0 = 749 \pm 20$ K. The present T_0 value is in rough agreement with the data obtained from measurements of the dielectric constant,[22] the specific heat,[50] and the phenomenological thermodynamic calculation.[49] The soft TA modes at the midpoint (0.25,0.25,0.25) and the R point are rather insensitive to temperature between 793 and 1173 K, as will be shown in Sec. III B. As shown in Fig. 2, the phonon dispersion relations for tetragonal $PbTiO_3$ present no evidence for an instability at 295 K.[7] Consequently, the softening of the TO modes toward the Γ point plays a dominant role in the structural phase transition in $PbTiO_3$.

The TO Γ_{15} mode should split into the TO A_1 and E modes in the tetragonal phase. The TO A_1 mode at the Γ point is responsible for the spontaneous polarization **P** along the [0,0,1] direction. The degenerated TO Δ_5 branch in the cubic phase corresponds to the TO-like Δ_1 and TO Δ_2 branches along the [1,0,0] direction in the tetragonal phase. The TO Δ_2, TO-like Δ_1, Σ_1, and Σ_2 branches become hard considerably near the zone center at 295 K. At the Γ point, the TO phonon energy for the A_1 mode is 18.1 meV, and that for the E mode is 11.5 meV at 295 K.[7] These TO A_1 and E mode energies are in good agreement with Raman scattering data.[51,52] Dielectric measurements for tetragonal $PbTiO_3$ show that the value for the dielectric constant ε_{11} perpendicular to the spontaneous polarization **P** is three times as large as that for ε_{33} parallel to **P** at room temperature[53] (namely, $\varepsilon_{11} = 101$, and $\varepsilon_{33} = 34$ at 12 MHz.) The LST relation predicts that the square of the phonon energy E_0^2 for the TO A_1 mode is inversely proportional to ε_{33}. Similarly, E_0^2 for the E mode is inversely proportional to ε_{11}. The energy difference between A_1 and E modes is consistent with the relation $\varepsilon_{33} < \varepsilon_{11}$ via the LST relation.

Our results for the TO Γ_{15} mode are consistent with the previous study by Shirane *et al.*,[6] as shown in Fig. 6. In contrast, Kempa *et al.*[9] reported that the zone-center energy of the TO branches in $PbTiO_3$ is 5.5 meV at 775 K ($T_c + 12$ K). A micro-Raman scattering study of cubic $PbTiO_3$ also indicated that the soft mode energy approaches 5.2 meV at 775 K.[54] A likely explanation for this discrepancy is that Pb vacancies or impurity defects in the sample used in Ref. 9 contribute to incomplete softening of the TO Γ_{15} mode above T_c.

2. *Zone-boundary TO modes*

The TO phonon branches in Fig. 3 are nearly isotropic in the cubic phase. The difference in the TO phonon energy is relatively small among the X_5, M_3', M_3, and R_{15} modes. The TO Σ_4 branch in the cubic phase becomes flat away from the zone center. As shown in Fig. 2(d), the flat TO Σ_4 branch toward the M point (0.5,0.5,0) is quite different from the upward TO-like Σ_1 branch in the tetragonal phase. In particular, the energy of the TO M_3' mode at 18.5 meV in the cubic phase is considerably lower than the corresponding energy of the TO-like B_2 mode at 29.5 meV in the tetragonal phase.[7] The TO M_3' mode represents the displacement of the Ti and O_1 atoms along the [0,0,1] direction, as listed in Table I. The large spontaneous polarization **P** appears to stiffen the TO-like B_2 mode at the M point in the tetragonal phase.

The TO Δ_5 branch along [1,0,0] in the cubic phase splits into the TO Δ_2 and TO-like Δ_1 modes in the tetragonal phase.

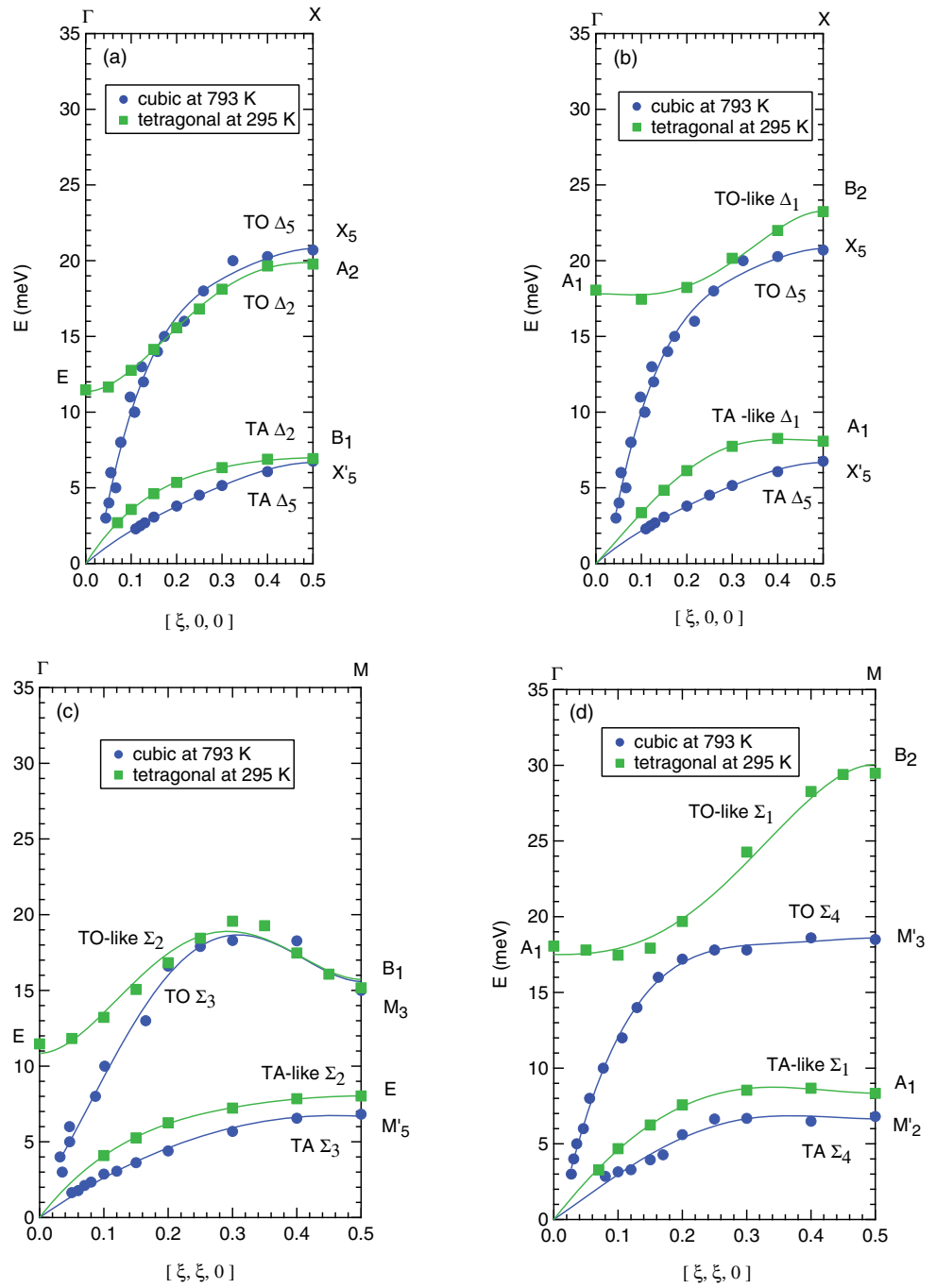

FIG. 2. (Color online) Comparison of phonon dispersion curves in cubic and tetragonal $PbTiO_3$. The tetragonal data at 295 K is taken from Ref. 7. Solid lines are guides to the eye.

It should be noted in Fig. 2 that the TO Δ_5 branch in the range $\xi \geqslant 0.15$ is in good agreement with the TO Δ_2 mode with [0,1,0] polarization. Furthermore, the TO Σ_3 branch with $[1,\bar{1},0]$ polarization in the range $\xi \geqslant 0.2$ is in agreement with the corresponding TO Σ_2 branch in the tetragonal phase. Both TO M_3 and TO B_1 modes at the M point represent the rotation of the oxygen octahedron around the [0,0,1] direction. Therefore, the spontaneous polarization **P** along [0,0,1] has little effect on the TO branches with polarization perpendicular to [0,0,1] away from the zone center.

The phonon dispersion relations in tetragonal $PbTiO_3$ (Ref. 7) are in good agreement with the first-principles calculations for the zone-center and zone-boundary phonon energies.[11] This agreement reflects the fact that the lattice dynamics of ground-state tetragonal $PbTiO_3$ is essentially temperature independent below 300 K. The present phonon dispersion relations for cubic $PbTiO_3$ provide support for the calculated instability of the Γ_{15} and R_{25} modes.[13,46,55] Like the M_3 mode, the R_{25} mode denotes the rotational motion of oxygen octahedra. There is, however, a marked difference

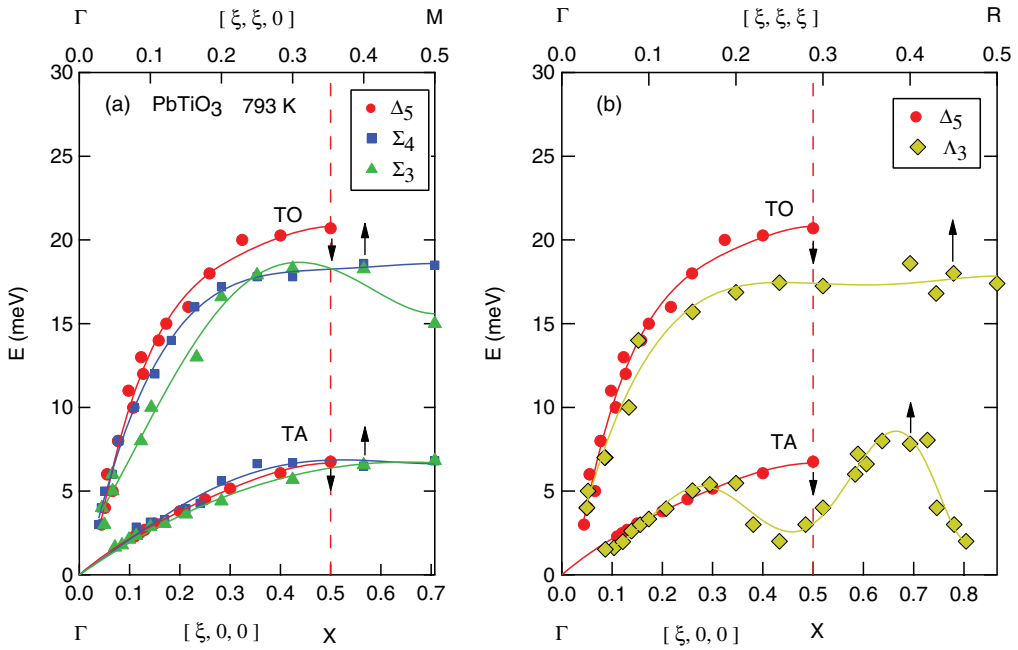

FIG. 3. (Color online) Comparison of the Δ_5, Σ_3, Σ_4, and Λ_3 branches in cubic $PbTiO_3$ at $T = 793$ K. Solid lines are guides to the eye.

between the soft R_{25} and stable M_3 modes in Fig. 1. The observed difference is in contrast with the prediction that the flat $R_{25} - M_3$ branch becomes unstable in the cubic phase.[13] As shown in Fig. 2(a), the energy of the TO X_5 mode at 793 K is nearly equal to that of the TO A_2 mode at 295 K. The temperature-independent TO mode at the X point is inconsistent with the unstable TO X_5 mode studied by first-principles calculations.[13]

B. TA modes

1. TA Δ_5, Σ_3, and Σ_4 modes

Figure 3 demonstrates the isotropic character of the TA Δ_5, Σ_3, and Σ_4 phonon branches at 793 K. Previously, Shirane *et al.*[6] reported a dip in the TA Δ_5 curve around $q = 0.1$, which was attributed to the harmonic coupling with the soft TO mode. In Fig. 7, the present TA Δ_5 branch is compared with the previously reported data.[6,9] The energies of TA Δ_5 mode between $q = 0.15$ and 0.3 determined by Shirane *et al.*[6] are higher than the corresponding data of this study and Kempa *et al.*[9] Our results show that the TA Δ_5 branch has a normal phonon dispersion in the entire q range, in agreement with the data of Kempa *et al.*[9] These results do not support the picture that the softening of the TO Δ_5 mode has influence on the TA Δ_5 mode in the small q region.

It should be noted in Fig. 8(a) that the TA Δ_5 branch at 1173 K ($T_c + 410$ K) is higher than that at 793 K. In contrast, Fig. 2 shows that the TA Δ_5 branch at 793 K is considerably lower than the TA-like Δ_1 or the TA Δ_2 branch at 295 K. Similarly, the TA Σ_3 and Σ_4 branches at 793 K are lower than the TA-like Σ_2 and Σ_1 branches at 295 K, respectively. Therefore, the soft TA modes in the entire q range are closely associated with the occurrence of the phase transition. The TA branches in cubic $PbTiO_3$ are mainly governed by the Pb and O atom motion, except for the TA Λ_3 branch around the midpoint (0.25,0.25,0.25) and the R point. In particular, the TA M_2' mode is expressed in terms of the displacement of Pb along [0,0,1]. The Pb participation in TA modes is due to the large atomic mass of Pb at the A site. The energies of the TA X_5', M_5', and M_2' modes in the cubic phase are lower than those of the TA-like A_1, E, and A_1 modes in the tetragonal phase, respectively. These results suggest that the force constants between Pb and O atoms soften as the transition temperature is approached.

Table II shows the elastic constants C_{ij} derived from the initial slopes of TA branches in $PbTiO_3$. The piezoelectricity is induced in tetragonal $PbTiO_3$. In this paper, C_{ij} and C_{ij}^P for the tetragonal phase denote the elastic constants at constant field and the elastic constants at constant polarization, respectively. The distinction is unnecessary in cubic symmetry. In the cubic phase, the slope of the TA Δ_5 and Σ_4 branches gives C_{44}, whereas that of the TA Σ_3 branch yields $0.5(C_{11} - C_{12})$. The elastic constant C_{44} is nearly equal to $0.5(C_{11} - C_{12})$ at 793 K, indicating that cubic $PbTiO_3$ is elastically isotropic. In tetragonal $PbTiO_3$ the elastic constant C_{66}^E is much higher than C_{44}^E, although C_{44}^E is nearly equal to $(C_{11}^E - C_{12}^E)$.[7] Table II indicates that both C_{44} and $0.5(C_{11} - C_{12})$ soften significantly toward T_c. Generally the elastic constants are expected to decrease with increasing temperature, due to an anharmonic effect. In contrast, the elastic constant C_{44} in the cubic phase exhibits softening below 1173 K.

2. TA Λ_3 mode

Figure 8(b) shows that the TA Λ_3 branch exhibits two minima around the midpoint (0.25,0.25,0.25) and the R point at 793 K and 1173 K. Typical constant-$\mathbf{Q}$ scans at $(1 + H, 1 + H, 1 - H)$ are shown in Fig. 9. A well-defined TA Λ_3 mode at $q = (0.08, 0.08, 0.08)$ is in marked contrast to overdamped modes at $q = (0.25, 0.25, 0.25)$ and (0.5,0.5,0.5). Figure 9(a) clearly shows that the long-wavelength TA Λ_3

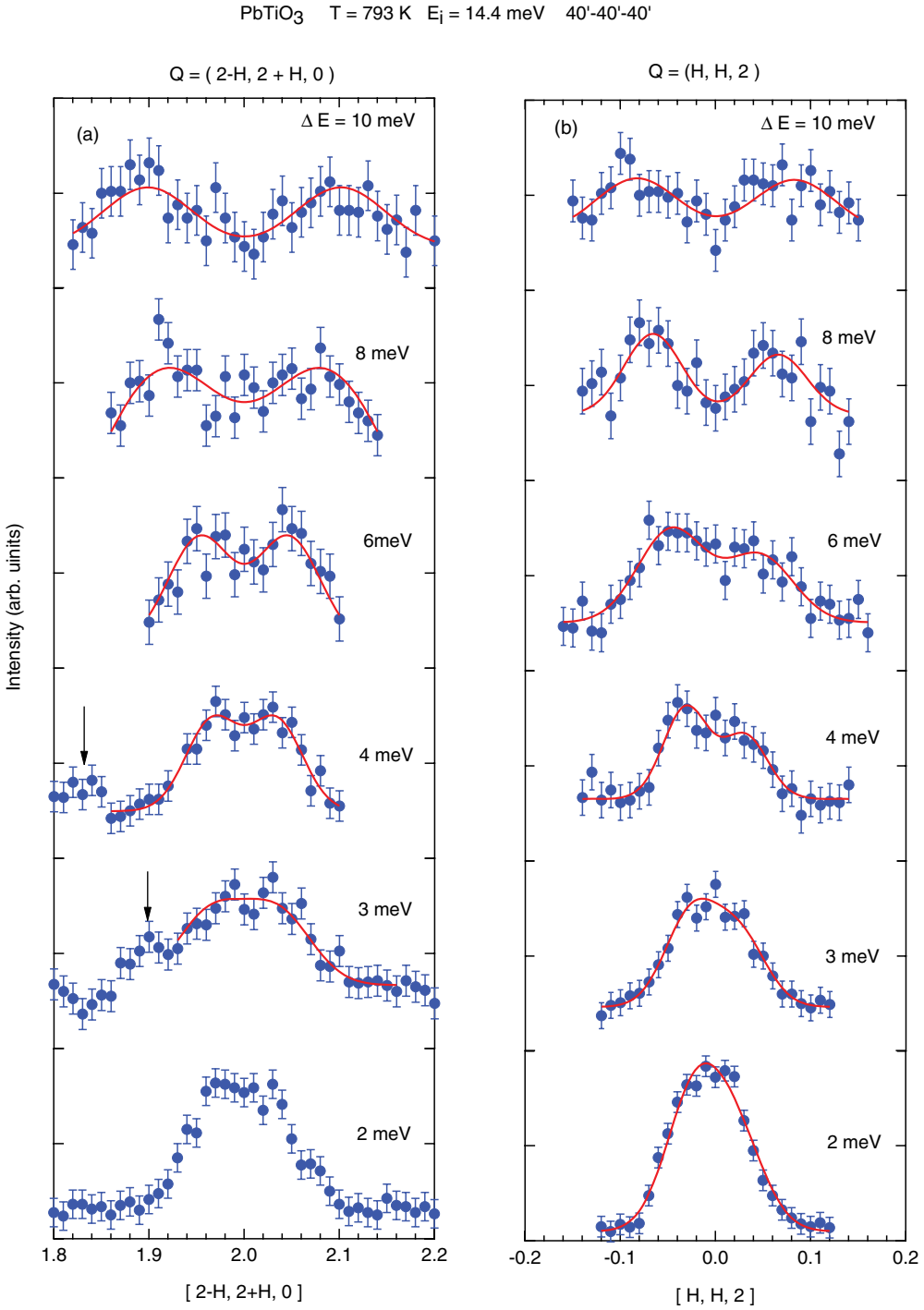

FIG. 4. (Color online) Constant-E scans for $PbTiO_3$ along (a) the $[2-H,2+H,0]$ and (b) the $[H,H,2]$ directions at $T = 793$ K. The arrows indicate the TA Σ_3 phonon peaks. The solid lines are Gaussian fits to the data.

mode becomes hard at 1173 K, as is the case for the TA Δ_5 mode. Constant-E scans through the midpoint and the R point are plotted in Figs. 10 and 11, respectively. The TA mode anomaly toward the R point results from the softening of the R_{25} rotation mode of oxygen octahedra. The TA R_{25} and the midpoint Λ_3 modes are rather insensitive to temperature up to 1173 K. The anomaly in the TA Λ_3 branch at the midpoint is quite different from the normal phonon dispersion for the TA Δ_5, Σ_3, and Σ_4 branches. The covalent nature of the Pb and O atoms appears to play an important role in the double minima of the TA Λ_3 branch. The broad minimum around (0.25,0.25,0.25) suggests a tendency toward forming a fourfold periodicity along the [1,1,1] direction. A possible interpretation is that the octahedron rotation of successive oxygen layers follows the sequence of same, same, opposite, and opposite senses.

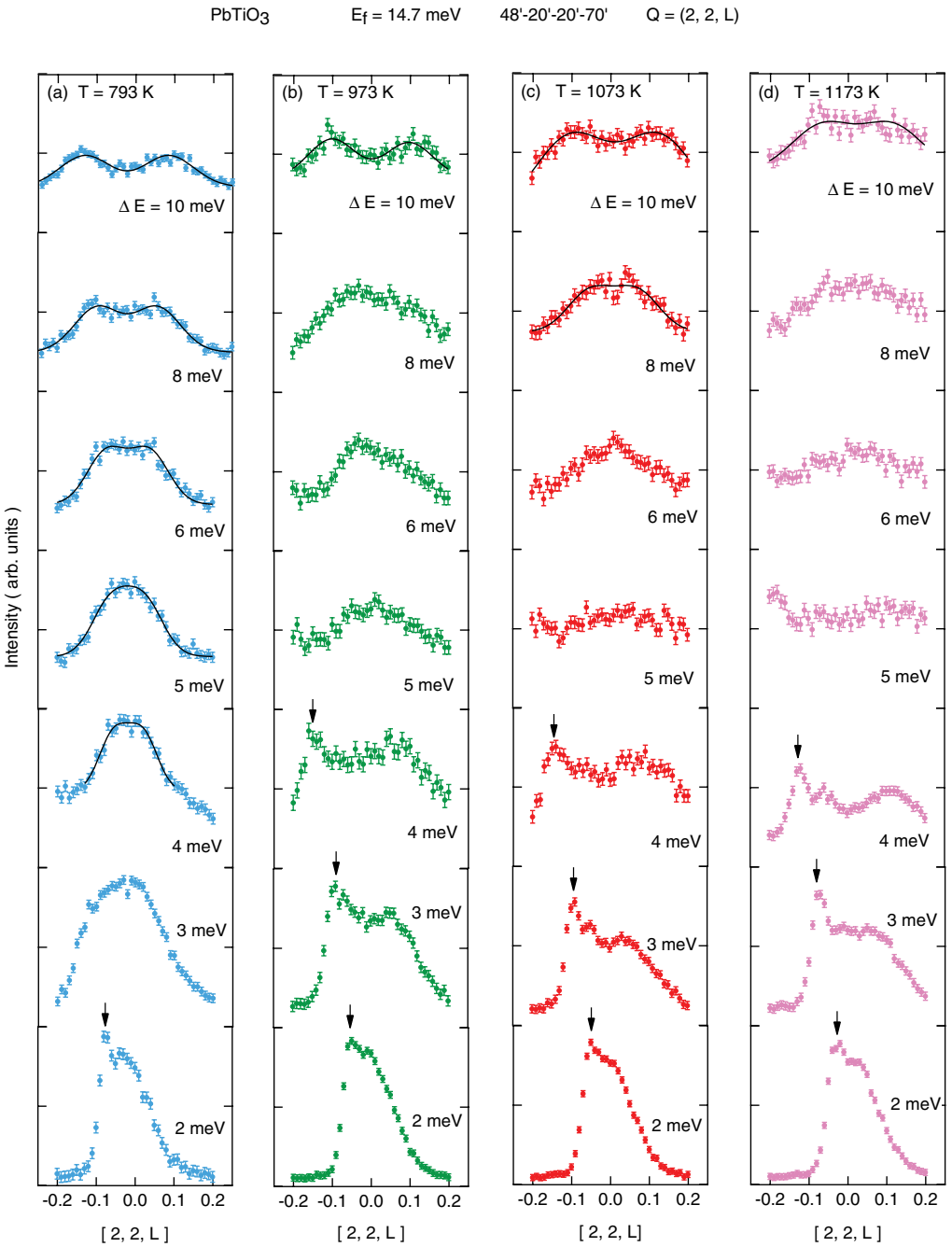

FIG. 5. (Color online) Constant-E scans in $PbTiO_3$ along the $[2,2,L]$ direction at (a) 793 K, (b) 973 K, (c) 1073 K, and (d) 1173 K. The solid lines are Gaussian fits to the TO phonon data. The arrows indicate the TA Δ_5 phonon peaks.

IV. COMPARISON WITH SIMPLE AND Pb-BASED COMPLEX PEROVSKITES

A. Comparison with simple perovskites

In Table III, we summarize the soft TO modes for simple perovskites ABO_3 observed by inelastic neutron scattering. Generally, the soft mode behavior in ABO_3 has been characterized by a geometric tolerance factor, $t = (r_O + r_A)/\sqrt{2}(r_O + r_B)$, where r_O, r_A, and r_B are the ionic radii of the O, A, and B atoms, respectively. Both $BaTiO_3$ and $KNbO_3$ with $t \geqslant 1.06$ have only the ferroelectric instability. The zone-center soft mode for $BaTiO_3$[10] and $KNbO_3$[57] is anisotropic and overdamped. For $BaTiO_3$, the Ti atom at the center of O octahedron is covalently bonded with 6 O atoms, and the hybridization of Ti $3d$ and O $2p$ orbitals weakens the short-range repulsions.[4,5,13,66] Furthermore, the motion of the Ba atom at the A site is essentially not involved in the soft Γ_{15} mode in $BaTiO_3$. Thus, the Ti displacement along the Ti-O-Ti chain is responsible for the anisotropic soft TO mode at the Γ point in $BaTiO_3$. The zone-center soft TO mode in $KNbO_3$ is also explained in terms of the motion of the Nb and O atoms along the $\langle 100 \rangle$ directions.[67]

Our results for cubic $PbTiO_3$ show that the soft TO mode toward the Γ point is isotropic and well defined. In $PbTiO_3$,

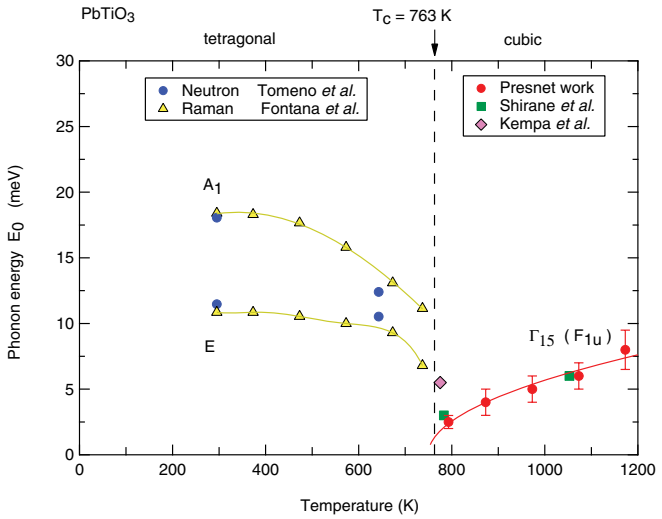

FIG. 6. (Color online) Zone-center TO phonon energy E_0 in $PbTiO_3$ as a function of temperature. Above T_c the present data are compared with the neutron scattering data taken from Refs. 6 and 9. The solid line above T_c is a least-squares fit to the data as described in the text. Below T_c the circles represent the neutron scattering data from Ref. 7, and the triangles refer to the Raman scattering data from Ref. 51.

the Pb 6*s* state at the *A* site is hybridized with the O 2*p* state. The Pb atom motion is rather isotropic, because the Pb atom is surrounded by 12 O nearest neighbors. Theoretical calculations[13,46] show that the soft TO mode at Γ in $PbTiO_3$ consists of the two components: (1) the displacement of the Pb atom against the O atoms in the Pb-O planes, and (2) the Ti atom motion against the O atoms along the Ti-O-Ti chain directions. The isotropic and well-defined soft mode toward Γ indicates the importance of the Pb atom motion in $PbTiO_3$.

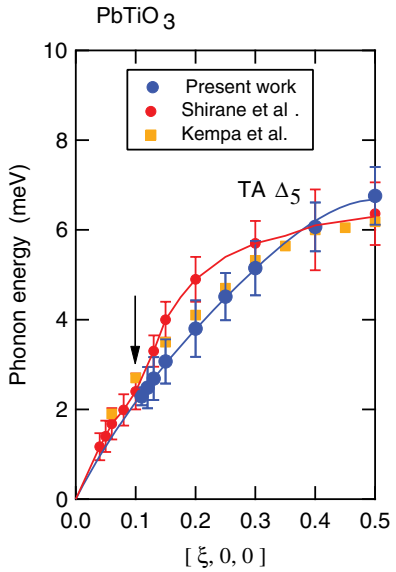

FIG. 7. (Color online) TA Σ_5 branch in $PbTiO_3$ at 793 K in comparison with the data of Shirane *et al.* (Ref. 6) at 783 K and that of Kempa *et al.* (Ref. 9) at 775 K. The arrow denotes the dip reported in Ref. 6.

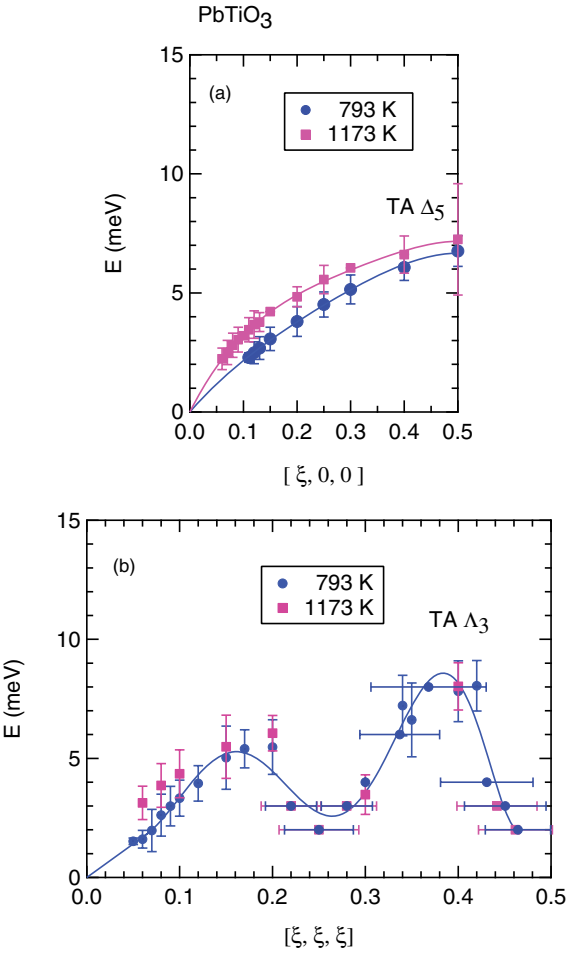

FIG. 8. (Color online) Temperature dependence of (a) the TA Δ_5 branch and (b) the TA Λ_3 branch in cubic $PbTiO_3$. Each solid circle and the attached bar refer to the phonon peak and its FWHM, respectively. Solid lines are guides to the eye.

For cubic $BaTiO_3$, the TO Σ_3 and TO Λ_3 branches stiffen rapidly toward the end points when compared to the TO Σ_4 and Δ_5 branches.[10,68] In $BaTiO_3$, the normal modes at the end points of the TO Σ_3 and TO Λ_3 branches are the M_5' and R_{15} modes, respectively.[13,66] In contrast, the normal modes at the end points of the TO Δ_5 and TO Σ_4 branches for $BaTiO_3$ remain the same as for $PbTiO_3$. In $BaTiO_3$, the X_5 and M_3' modes are dominated by the Ti displacement against the O atoms, whereas the M_5' and R_{15} modes are dominated by the Ba displacement against the O atoms. The ionic nature of the Ba atom results in the strong force constants between

TABLE II. Elastic constants (in 10^{11} N/m^2) for $PbTiO_3$ estimated from the initial slope of the phonon dispersion curves. The tetragonal data are taken from Ref. 7.

	Tetragonal	Cubic	Cubic
T (K)	295	793	1173
$0.5(C_{11}-C_{12})$	0.63 ± 0.01	0.34 ± 0.06	
C_{44}^P	0.80 ± 0.01		
C_{44}	0.72 ± 0.02	0.32 ± 0.02	0.94 ± 0.05
C_{66}	1.06 ± 0.02		

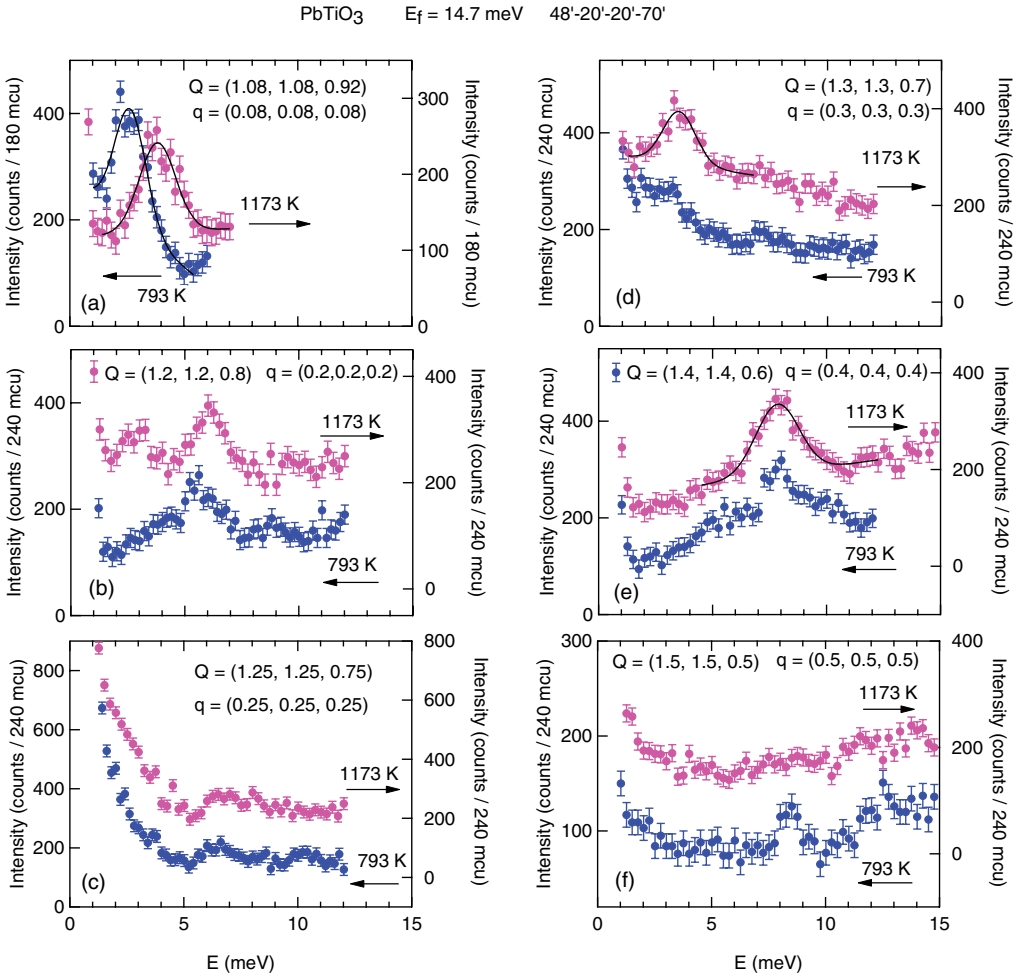

FIG. 9. (Color online) Typical constant-**Q** scans in $PbTiO_3$ for the $[\xi,\xi,\xi]$ direction at $T = 793$ and 1173 K. Neutron intensity is presented in the units of counts per monitor count unit (mcu), with 1 mcu corresponding to a counting time of ~1 s. The solid lines are Gaussian fits to the data.

A and O atoms. Therefore, the anisotropic dispersion of TO branches in the entire q range reflects the distinction between the ionic A-O and and the covalent B-O bonding states in $BaTiO_3$. With the exception of the TA Λ_3 mode, both the TA and the TO branches in cubic $PbTiO_3$ are nearly isotropic in a wide q range. The TA Δ_5, Σ_3, and Σ_4 branches are governed by the Pb motion due to its large atomic mass. The TO X_5 and M_3' modes in Fig. 3 are dominated by the Ti atom motion. In contrast, the TO M_3 mode represents the rotation of the oxygen octahedra and the TO R_{15} mode involves the Pb displacement. The small energy difference at zone boundaries indicates that the ratio of the atomic force constant to the atomic mass remains approximately constant in cubic $PbTiO_3$. The isotropic TO branches away from Γ are largely due to the Pb-O hybridization and the large atomic mass of Pb, in comparison with the anisotropic TO branches in $BaTiO_3$.

The phonon dispersions for $PbTiO_3$ demonstrate the coexistence of the soft Γ_{15} and R_{25} modes, as shown in Fig. 1. Table III indicates that the R_{25} mode softening in ABO_3 exists on the condition $t \leqslant 1.03$. A weak instability at R has been theoretically predicted for $PbTiO_3$ with $t = 1.03$.[13,46,55] There are two oxygen rotational modes, R_{25} and M_3, in ABO_3. As shown in Fig. 1, the TO M_3 mode remains stable in cubic $PbTiO_3$. The M_3 mode in $SrTiO_3$ shows a slight softening,[63] whereas the M_3 mode in $NaNbO_3$ exhibits a significant softening.[65] Thus these experimental results suggest that the small A-site ion is essential to the simultaneous softening of R_{25} and M_3 modes.

To date there have been only a few reports on the softening of the TA phonon curves in ABO_3. For $KTaO_3$, the TA Δ_5 and Σ_4 branches exhibit softening away from the zone center on cooling.[60–62,69] However, ultrasonic velocity measurements in $KTaO_3$ show that the elastic constants C_{11} and C_{44} increase gradually with decreasing temperature.[70] The abnormal behavior of the TA Δ_5 branch in $KTaO_3$ vanishes in the long-wavelength region. On the other hand, the TA Λ_3 and Σ_3 branches in $KTaO_3$ behave normally.[69] The displacement of Ta atoms dominates the TA Δ_5 branch toward X and the TA Σ_4 branch toward M, whereas that of K atoms is responsible for the TA Σ_3 mode toward M. It follows that the Ta atom motion is related to the softening of the TA modes. Axe *et al.*[60] interpreted that the quasiharmonic coupling between TO and TA modes gives rise to the anisotropic softening of the TA

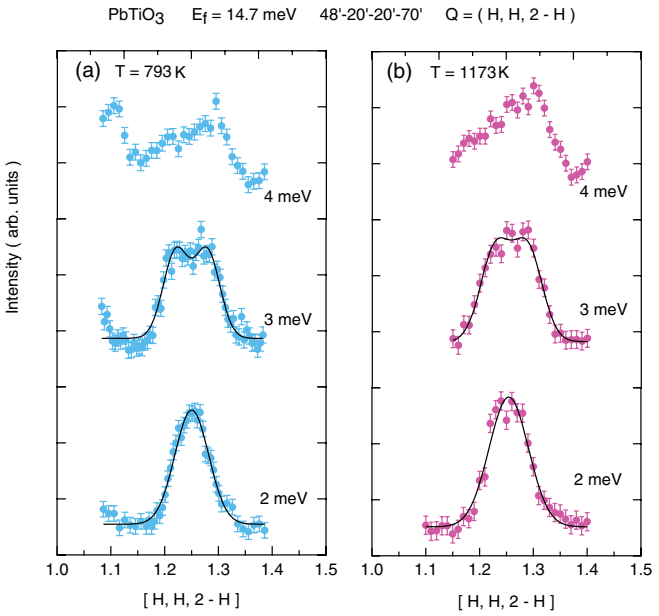

FIG. 10. (Color online) Constant-E scans in $PbTiO_3$ for the Λ_3 mode through the midpoint (0.25,0.25,0.25) at (a) 793 K and (b) 1173 K. The solid lines are Gaussian fits to the data.

phonon in $KTaO_3$. There is a significant difference in the soft TA modes between $PbTiO_3$ and $KTaO_3$. As shown in Figs. 2 and 8, the TA Δ_5, Σ_3, and Σ_4 branches for $PbTiO_3$ soften in the entire q range toward T_c. Furthermore, the TA Λ_3 mode in

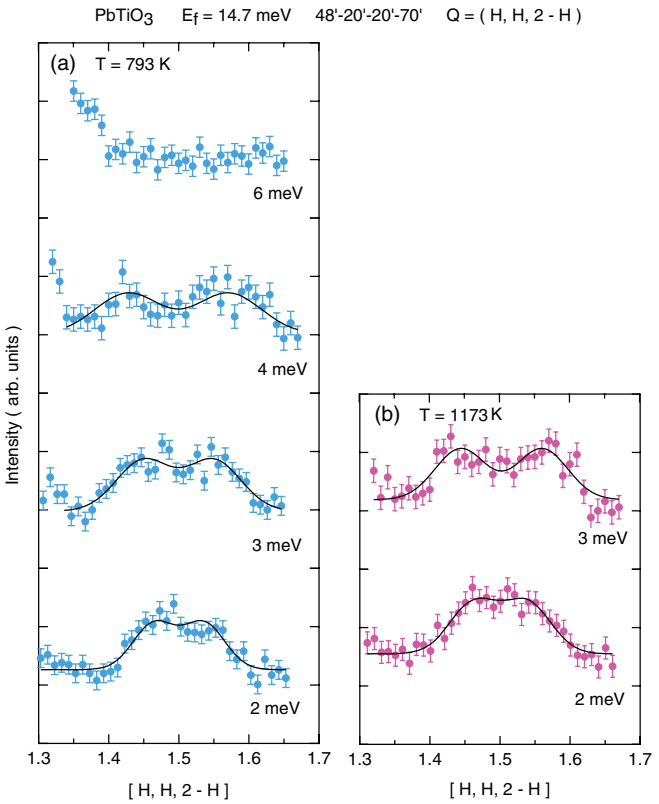

FIG. 11. (Color online) Constant-E scans in $PbTiO_3$ for the Λ_3 mode through the R point at (a) 793 K and (b) 1173 K. The solid lines are Gaussian fits to the data.

TABLE III. Soft modes, and tolerance factor t for simple perovskite ABO_3. Soft modes were observed by inelastic neutron scattering.

ABO_3	Soft modes	t	Reference
$BaTiO_3$	Γ_{15}	1.07	10, 56
$KNbO_3$	Γ_{15}	1.06	57, 58, 59
$KTaO_3$	Γ_{15}	1.06	60, 61, 62
$PbTiO_3$	Γ_{15}, R_{25}, Λ_3 at (0.25,0.25,0.25)	1.03	Present work
$SrTiO_3$	Γ_{15}, R_{25}	1.01	63, 64
$NaNbO_3$	Γ_{15}, M_3, R_{25}	0.97	65

$PbTiO_3$ softens in the long-wavelength region toward T_c. The elastic constants for $PbTiO_3$ decrease toward T_c, as shown in Table II. For $PbTiO_3$ the softening of the TA branches in the entire q range cannot be explained by the coupling with the soft TO mode near the zone center. As stated previously, the softening of the TA branches in $PbTiO_3$ can be attributed to the variation of Pb-O force constants with temperature.

To our knowledge, this is the first report of the softening of the Λ_3 mode at the midpoint (0.25,0.25,0.25) in ABO_3. The covalent nature of the A-site atom seems responsible for the unstable TA Λ_3 mode around the midpoint. Lead zirconate $PbZrO_3$ is another Pb-based simple perovskite with $t = 0.97$. For cubic $PbZrO_3$, Cochran and Zia[71] proposed the four unstable modes: Γ_{15}, Σ_3 at (0.25,0.25,0), M_5' and R_{25}. A complicated crystal structure of $PbZrO_3$ below approximately 505 K is closely related to the condensation of the soft TO Σ_3 and R_{25} modes.[72,73] In contrast, $PbTiO_3$ remains the tetragonal phase at low temperatures. Thus our finding on the midpoint softening for $PbTiO_3$ is quite different from the unstable TO Σ_3 mode at (0.25,0.25,0) for $PbZrO_3$. The recent first-principles calculations present a variety of soft modes for $PbTiO_3$ and $PbZrO_3$.[13] For example, the TA Λ_3 branch for $PbZrO_3$ away from the zone center is more unstable than that for $PbTiO_3$. The displacement of Pb and O atoms dominates the TA Λ_3 branch in $PbTiO_3$ and $PbZrO_3$. Obviously, it is desirable that the phonon dispersion relations for $PbZrO_3$ are determined experimentally.

B. Comparison with Pb-based complex perovskite

Figure 12 presents a comparison of the phonon dispersion relations for cubic $PbTiO_3$ with those for cubic PZN measured at 423 K.[31] For the relaxor PZN, the TO Δ_5 branch drops toward the characteristic wave vector $q_{wf} \sim 0.1$ r.l.u. and then merges into the corresponding TA branch. The TO Σ_3 branch in PZN displays similar behavior. The sharp drop in the TO branches toward q_{wf} for PZN is a typical example of the waterfall phenomenon. The soft mode toward Γ in $PbTiO_3$ is distinct from the waterfall phenomenon toward q_{wf} in PZN-xPT and PMN-xPT.[30–40]

It is important to note in Fig. 12 that the energies of the TO Δ_5 branch for $PbTiO_3$ are considerably higher than those for PZN in the entire q range. Table IV clearly shows that the X-point TO phonon energy for $PbTiO_3$ is much higher than the corresponding X-point energies for PZN, PMN, or $PbZr_{1-x}Ti_xO_3$ (PZT) with $x \sim 0.475$. The TO X_5 mode in these materials is governed by the B-site and O atoms. Here

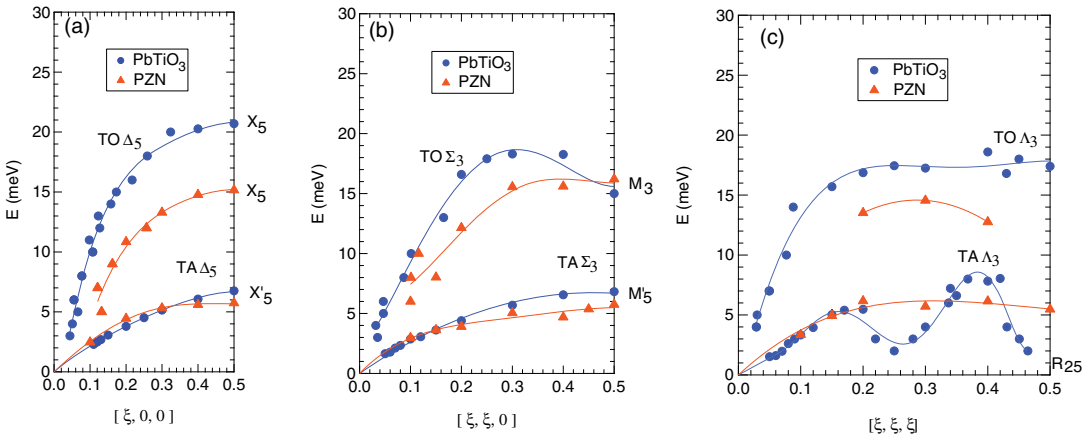

FIG. 12. (Color online) Comparison of phonon dispersion curves for $PbTiO_3$ at 793 K with those for PZN at 423 K. The PZN data is taken from Ref. 31. Solid lines are guides to the eye.

we will focus on a comparison with the phonon dispersion relations for PZN at 423 K.[31] The energy of the M_3 oxygen rotational mode for $PbTiO_3$ is nearly equal to that for PZN. Except for the M point, the energies of the TO Σ_3 branch for $PbTiO_3$ are higher than those for PZN. A similar difference in the TO Λ_3 modes is found between $PbTiO_3$ and PZN. The replacement of the B-site atom has a strong influence of the TO phonon branch in the Pb-based perovskites. For example, the average mass of the B-site atom in PZN is 1.75 times that of Ti in $PbTiO_3$. Therefore, the reduction of the TO X_5 mode energy is roughly explained in terms of the square root of the B-atom mass. The force constants between Ti and O atoms for $PbTiO_3$ appear to be comparable to or slightly weaker than those between the B-site and O atom for PZN.

It should be noted that the TA Δ_5 branch for $PbTiO_3$ is slightly higher than for PZN. The corresponding TO Δ_5 branch for PZN is much lower than that for $PbTiO_3$ in the entire q region. For Pb-based relaxors, the q_{wf} position refers to the merging point of TO and TA branches. The change in the X-point energy of the TO Δ_5 branch should shift the q_{wf} value. For cubic $NaNbO_3$, the soft TO Σ_4 branch merges into the corresponding TA branch near $q = [0.15,0.15,0]$.[65] The steep drop in the TO Σ_4 mode for $NaNbO_3$ is similar to the waterfall phenomenon observed for the Pb-based relaxors. Moreover, the waterfall phenomenon is found for the system PMN-0.6PT, which exhibits conventional ferroelectric behavior.[39] In view of these results, it seems reasonable to assume that the q_{wf} position is independent of the size of polar nanoregions in relaxors.

For cubic $PbTiO_3$, the TO Σ_3, TO Σ_4, TA Σ_3, and TA Σ_4 branches are very stable at the M point, as shown in Fig. 1. These results for $PbTiO_3$ are distinct from the phonon instability at the M point in PMN and PZT.[41,45] For the relaxor PMN, the TO branches propagating along [1,1,0] and [1,1,1] become soft toward the M and R points, respectively.[41] Furthermore, the soft modes in PMN lie along the zone edge between $q = (0.5,0.5,0)$ and $q = (0.5,0.5,0.5)$. The zone-boundary soft modes are assigned as the M_2' and R_{15} modes.[41] As seen from Table I, the displacement of B-site atoms is not involved in these modes. A possible explanation for the zone-boundary soft modes is that the disorder at the B site weakens the force constant between Pb and O atoms in PMN. For PZT with $x \sim 0.475$, the M_5' zone-boundary mode softens significantly on cooling from the paraelectric to monoclinic phase, whereas the M_2' mode does not show any appreciable change with temperature.[45] Hlinka *et al.*[45] interpreted that the soft mode behavior at the M point in PZT originates from the nanoscale structural inhomogeneity. Further studies are needed to clarify the origin of the zone boundary softening in the Pb-based perovskites.

TABLE IV. Phonon energies at X (0.5,0,0) for Pb-based perovskites.

Materials	TA (meV)	TO (meV)	T (K)	Reference
$PbTiO_3$	6.8 ± 0.1	20.7 ± 0.4	793	Present work
PZN	5.7	15.2	423	31
PMN	5.6	15.8	800	74
PZT with $x \sim 0.475$	5.7	13.2	740	45

For PZN and PMN-xPT, the zone center TO mode emerges in the temperature range where the waterfall phenomenon is suppressed. In Fig. 13, the temperature dependence of the zone-center TO phonon energy E_0 for $PbTiO_3$ is compared with that for PZN,[38] PMN,[35,36,74] and PMN-0.6PT.[39] On the high-temperature side, the zone-center TO mode for PMN is found above the Burns temperature $T_d \sim 620$ K. At 1100 K, the zone-center TO phonon energy E_0 for PMN is nearly equal to that for $PbTiO_3$. This indicates that the long-wavelength motion of Pb and O atoms in PMN at $T \sim T_d + 480$ K is similar to that for $PbTiO_3$ at $T = T_c + 337$ K. For $PbTiO_3$, the zone-center TO phonon energy E_0 softens as the Curie temperature is approached from above. As stated in Sec. III A, the temperature dependence of E_0 for cubic $PbTiO_3$ can be accounted for by the Curie-Weiss law via the LST relation. In contrast, the zone-center TO phonon energy E_0 in PMN decreases very slowly on cooling down to $T_d \sim 620$ K. Above T_d, the dielectric constant in PMN follows the Curie-Weiss law $\varepsilon = C/(T - T_0)$ with the extrapolated Curie temperature $T_0 \sim 400$ K.[26] Furthermore, the dielectric constant ε in PMN is frequency independent above T_d. In view of the LST relation and the observed dielectric constant ε, one can expect that the

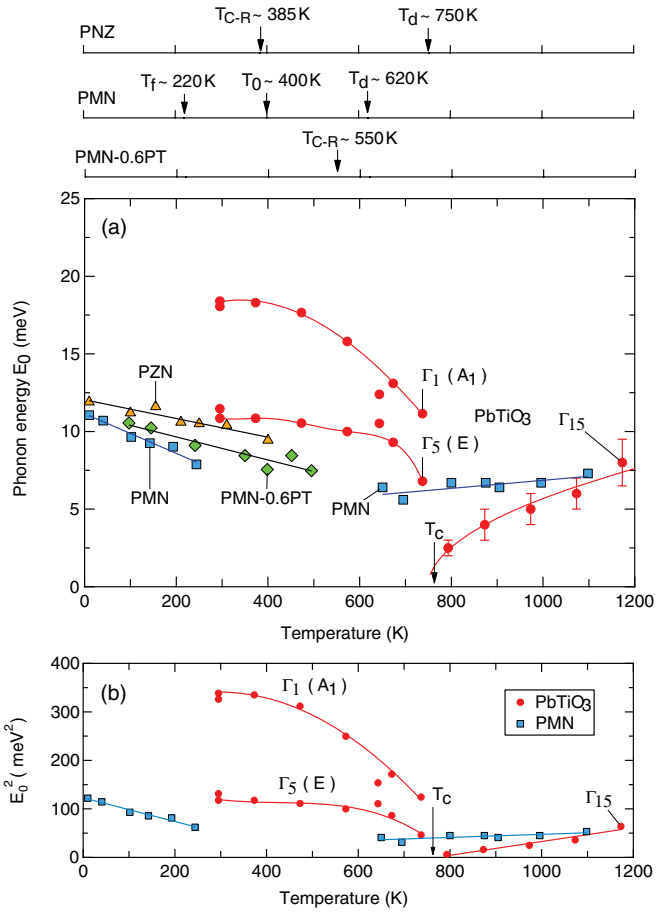

FIG. 13. (Color online) (a) Zone-center TO phonon energy E_0 for $PbTiO_3$, PNZ, PMN, and PMN-0.6PT as a function of temperature. The PZN data below $T_{C-R} \sim 385$ K are taken from Ref. 38, and the PMN data below $T_f \sim 220$ K and above $T_d \sim 620$ K are taken from Refs. 35 and 74. The PMN-0.6PT data below $T_{C-T} \sim 550$ K are obtained from Ref. 39. Solid lines are guides to the eye. (b) Square of zone-center TO phonon energy vs temperature for $PbTiO_3$ and PMN.

similar soft TO mode exists in PMN above T_d. Wakimoto *et al.*[36] interpreted that the weakly temperature dependent E_0 for PMN results from the Curie-Weiss behavior of ε, because the temperature-dependent part of E_0^2 above $T_d \sim 620$ K in Fig. 13(b) is proportional to $T - T_0$ with $T_0 \sim 400$ K. In contrast, hyper-Raman scattering experiments suggest a splitting of the lowest TO Γ_{15} mode in PMN between 520 and 750 K.[42] Al-Zein *et al.*[42] showed that the upper TO A_1 phonon energy determined by hyper-Raman scattering is in agreement with the TO phonon energy E_0 by inelastic neutron scattering.[33,35] They argued that the lower TO E_1 mode in PMN is responsible for the Curie-Weiss behavior of ε.[42] The TO mode splitting in PMN suggests that the polar nanoregions remain above $T_d \sim 620$ K. Further experimental studies are needed to understand the relation between the weakly temperature dependent E_0 and the Curie-Weiss behavior of ε above T_d.

The TO A_1 and E mode energies in tetragonal $PbTiO_3$ tend to saturate below about 400 K. Figure 13(b) shows that the relation $E_0^2 \propto (T_c - T)$ does not hold for the zone-center TO-A_1 mode in tetragonal $PbTiO_3$. In light of the LST relation, it is reasonable to expect that the inverse dielectric constant $1/\varepsilon_{33}$ for $PbTiO_3$ deviates considerably from the linear temperature dependence below T_c. For PMN, the zone-center TO mode recovers below the freezing temperature $T_f \sim 220$ K.[35,36] The zone-center TO modes are also found in rhombohedral PZN below the transition temperature $T_{C-R} \sim 385$ K and tetragonal PMN-0.6PT below $T_{C-T} \sim 550$ K.[38,39] On the lower temperature side, the square of the phonon energy E_0^2 for PZN, PMN, and PMN-0.6PT increases linearly with decreasing temperature.[35,36,38,39] By analogy with conventional ferroelectrics, the recovery of the zone-center TO mode in PZN and PMN has been considered to arise from the local spontaneous polarization in the polar nanoregions. It is clear from Fig. 13 that the TO phonon energy E_0 for PZN, PMN, and PMN-0.6PT is considerably lower than the TO E_0 energy for the A_1 mode in $PbTiO_3$. Moreover, the temperature dependence of E_0 for PZN, PMN, and PMN-0.6PT is different from that of E_0 for the A_1 mode in $PbTiO_3$. In PZN and PMN, the distribution of the polar nanoregions should affect the local spontaneous polarization and strain. In this circumstance, the zone-center energy E_0 in the polar nanoregions appears to be reduced compared with that for $PbTiO_3$.

Figure 12(c) shows the flat TA Λ_3 branch away from Γ for PZN. In addition, the TA Λ_3 branch in PMN has no anomaly around (0.25,0.25,0.25).[41] The disorder at the B site in relaxors tends to suppress the instability of fourfold periodicity along (1,1,1). The R_{25} mode for PZN is stable, although the average tolerance factor is smaller than unity. The TA phonon branches in cubic $PbTiO_3$ become soft toward T_c. The softening of the TA mode has been also observed for PMN between T_f and T_d.[40,75] Similar softening of the TA mode has been reported for the PZN-xPT relaxors.[76,77] Thus the Pb atom motion at the A site seems to play a crucial role in the acoustic softening near the structural phase transition.

V. CONCLUSION

We have determined the phonon dispersion relations for cubic $PbTiO_3$ at 793 K ($T_c + 30$ K). The phonon dispersion curves of the TO Δ_5, Σ_3, Σ_4, and Λ_3 modes fall sharply toward the zone center at 793 K. The energy of the TO Γ_{15} mode softens with decreasing temperature from 1173 K ($T_c + 410$ K) to 793 K. This temperature dependence is consistent with the Curie-Weiss law of the dielectric constant ϵ via the LST relation. The isotropic TO-phonon branches in cubic $PbTiO_3$ are compared with the anisotropic branches in tetragonal $PbTiO_3$ measured previously at 295 K.[7] In tetragonal $PbTiO_3$, the TO A_1 phonon energy at Γ is much higher than the TO E phonon energy. This can be understood in terms of the anisotropic dielectric constants, ϵ_{33} and ϵ_{11}.[53] The flat TO Σ_4 branch with [0,0,1] polarization toward M in the cubic phase is quite different from the corresponding upward TO-like Σ_1 branch in the tetragonal phase. The TO M_3' mode at (0.5,0.5,0) in the cubic phase represents the displacement of the Ti atom at (0.5,0.5,0.5) and the O_1 atom at (0.5,0.5,0) in the [0,0,1] direction. Therefore, the spontaneous polarization **P** along [0,0,1] stiffens the TO-like B_2 mode at M in the tetragonal phase. In contrast, the TO Σ_3 branch in the range $\xi \geqslant 0.2$ in the cubic phase is in agreement with the TO Σ_2 branch in the tetragonal phase. The TO M_3 rotational mode with $[1,\bar{1},0]$

polarization is very stable in cubic $PbTiO_3$. In addition, the TO Δ_5 branch in the range $\xi \geqslant 0.15$ in the cubic phase is in good agreement with the TO Δ_2 branch with [0,1,0] polarization in the tetragonal phase. Thus the spontaneous polarization **P** has little effect on the TO branches with polarization perpendicular to [0,0,1] away from the zone center.

The TA Λ_3 branch along $[\xi,\xi,\xi]$ in cubic $PbTiO_3$ shows significant softening around $\xi = 0.25$ and 0.5. The anomaly at the midpoint suggests the tendency toward forming the fourfold periodicity along the [1,1,1] direction, whereas the anomaly toward the R point is due to the softening of the R_{25} rotational mode. These two anomalies are rather insensitive to temperature up to 1173 K. The TA Δ_5 branch also softens gradually with decreasing temperature down to 793 K. The TA Δ_5 branch in the cubic phase at 793 K is lower than the TA-like Δ_1 and TA Δ_2 branches in the tetragonal phase at 295 K. Furthermore, the TA Σ_3 and Σ_4 branches at 793 K are lower than the TA-like Σ_2 and Σ_1 branches at 295 K, respectively. The elastic constants C_{44} and $0.5(C_{11} - C_{12})$ soften significantly toward T_c. Consequently, the gradual softening of TA branches along [1,0,0] and [1,1,0] is closely related to the structural phase transition at T_c. These results indicate that the force constants between Pb and O atoms soften around the phase transition. Although simultaneous softening of TA and TO modes occurs in the cubic phase near T_c, the tetragonal phase remains stable at low temperatures.[1] In particular, the phonon dispersion relations for tetragonal $PbTiO_3$ present the stability of the TA and TO modes along $[\xi,0,0]$, $[0,0,\zeta]$, and $[\xi,\xi,0]$ at 295 K.[7] Thus significant softening of the zone-center TO mode plays a major role in the single phase transition in $PbTiO_3$.

The isotropic dispersion of TO branches for cubic $PbTiO_3$ is in clear contrast to the anisotropic dispersion for cubic $BaTiO_3$.[10,68] For cubic $PbTiO_3$, the Pb atom motion participates in the isotropic and well-defined soft TO mode toward Γ. The isotropic nature of the TO branches is mainly due to the Pb-O hybridization and the large atomic mass of Pb. The softening of the TA Δ_5 branch for $PbTiO_3$ is essentially different from that for $KTaO_3$. For $KTaO_3$, the TA Δ_5 branch softens considerably away from Γ with decreasing temperature. In contrast to $PbTiO_3$, the elastic constant C_{44} for $KTaO_3$ shows no evidence for a phase transition at low temperatures.[70]

The soft TO mode toward Γ for $PbTiO_3$ is quite different from the sharp drop in the TO mode toward the characteristic wave vector q_{wf} of the order of 0.1 r.l.u. for the relaxors PZN and PMN.[31–33] The X-point energy of the TO mode for $PbTiO_3$ is much higher than the energies for the Pb-based perovskites PZN, PMN, and PZT.[31,45,74] The reduction of the TO X_5 mode energy can be explained in terms of the square root of the B-site atom mass. The stable M-point phonon modes for $PbTiO_3$ are distinct from the soft M_2' mode in PMN and the soft M_5' mode in PZT.[41,45] The zone-center TO phonon energy E_0 for PMN decreases slowly on cooling down to the Burns temperature $T_d \sim 620$ K, in marked contrast to the soft mode in cubic $PbTiO_3$. The zone-center TO phonon energy E_0 for PMN below the freezing temperature $T_f \sim 220$ K is considerably lower than the TO A_1 phonon energy for tetragonal $PbTiO_3$ at 295 K. The TO A_1 and E mode energies in tetragonal $PbTiO_3$ tend to saturate below about 400 K.[7,51] The temperature dependence of E_0 in tetragonal $PbTiO_3$ is quite different from that found for PMN and PZN on the lower temperature side.[35,36,38] The soft TA mode toward T_c in $PbTiO_3$ appears similar to the soft TA mode observed for the Pb-based relaxors around the dielectric-peak temperature $T_{\max}$.[40,75–77] These results indicate the involvement of Pb and O atom motion in the TA branches in $PbTiO_3$ and the Pb-based relaxors.

ACKNOWLEDGMENTS

We would like to thank M. A. Carpenter, Y. Ishii, J. M. Kiat, K. Kohn, J. L. Robertson, D. J. Singh, and H. Unoki for helpful discussions. This study was supported in part by the US-Japan Cooperative Program on Neutron Scattering. The work at Oak Ridge National Laboratory was supported by the Division of Scientific User Facilities, US Department of Energy Basic Energy Sciences.

*tomeno@gipc.akita-u.ac.jp

[1] H. Meštrić, R.-A. Eichel, T. Kloss, K.-P. Dinse, S. Laubach, S. Laubach, P. C. Schmidt, K. A. Schönau, M. Knapp, and H. Ehrenberg, Phys. Rev. B **71**, 134109 (2005).
[2] S. A. Mabud and A. M. Glazer, J. Appl. Cryst. **12**, 49 (1979).
[3] H. F. Kay and P. Vousden, Philos. Mag. Ser. **40**, 1019 (1949).
[4] R. E. Cohen, Nature (London) **358**, 136 (1992).
[5] R. E. Cohen and H. Krakauer, Phys. Rev. B **42**, 6416 (1990).
[6] G. Shirane, J. D. Axe, J. Harada, and J. P. Remeika, Phys. Rev. B **2**, 155 (1970).
[7] I. Tomeno, Y. Ishii, Y. Tsunoda, and K. Oka, Phys. Rev. B **73**, 064116 (2006).
[8] J. Hlinka, M. Kempa, J. Kulda, P. Bourges, A. Kania, and J. Petzelt, Phys. Rev. B **73**, 140101 (2006).
[9] M. Kempa, J. Hlinka, J. Kulda, P. Bourges, A. Kania, and J. Petzelt, Phase Transitions **79**, 351 (2006).
[10] J. Harada, J. D. Axe, and G. Shirane, Phys. Rev. B **4**, 155 (1971).
[11] A. García and D. Vanderbilt, Phys. Rev. B **54**, 3817 (1996).
[12] N. Choudhury, E. J. Walter, A. I. Kolesnikov, and C.-K. Loong, Phys. Rev. B **77**, 134111 (2008).
[13] P. Ghosez, E. Cockayne, U. V. Waghmare, and K. M. Rabe, Phys. Rev. B **60**, 836 (1999).
[14] J. Kuwata, K. Uchino, and S. Nomura, Ferroelectrics **37**, 579 (1981).
[15] J. Kuwata, K. Uchino, and S. Nomura, Jpn. J. Appl. Phys. **21**, 1298 (1982).
[16] S.-E. Park and T. R. Shrout, J. Appl. Phys. **82**, 1804 (1997).
[17] A. Lebon, H. Dammak, G. Calvarin, and I. O. Ahmedou, J. Phys.: Condens. Matter **14**, 7035 (2002).
[18] J. S. Forrester, E. H. Kisi, K. S. Knight, and C. J. Howard, J. Phys.: Condens. Matter **18**, L233 (2006).
[19] N. de Mathan, E. Husson, G. Calvarn, J. R. Gavarri, A. W. Hewat, and A. Morell, J. Phys.: Condens. Matter **3**, 8159 (1991).
[20] B. Noheda, D. E. Cox, G. Shirane, J. Gao, and Z.-G. Ye, Phys. Rev. B **66**, 054104 (2002).
[21] J.-M. Kiat, Y. Uesu, B. Dkhil, M. Matsuda, C. Malibert, and G. Calvarin, Phys. Rev. B **65**, 064106 (2002).

[22]J. P. Remeika and A. M. Glass, Mater. Res. Bull. **5**, 37 (1970).
[23]M. E. Lines and A. M. Glass, *Principles and Applications of Ferroelectrics and Related Materials* (Clarendon Press, Oxford, 1977).
[24]L. E. Cross, Ferroelectrics **151**, 305 (1994).
[25]E. V. Colla, E. Y. Koroleva, N. M. Okuneva, and S. B. Vakhrushev, Phys. Rev. Lett. **74**, 1681 (1995).
[26]D. Viehland, S. J. Jang, L. E. Cross, and M. Wuttig, Phys. Rev. B **46**, 8003 (1992).
[27]G. Burns and F. Dacol, Solid State Commun. **48**, 853 (1983).
[28]A. A. Bokov, Y.-H. Bing, W. Chen, Z.-G. Ye, S. A. Bogatina, I. P. Raevski, S. I. Raevskaya, and E. V. Sahkar, Phys. Rev. B **68**, 052102 (2003).
[29]D. Viehland, S. Jang, L. E. Cross, and M. Wuttig, Philos. Mag. B **64**, 335 (1991).
[30]P. M. Gehring, S.-E. Park, and G. Shirane, Phys. Rev. Lett. **84**, 5216 (2000).
[31]I. Tomeno, S. Shimanuki, Y. Tsunoda, and Y. Ishii, J. Phys. Soc. Jpn. **70**, 1444 (2001).
[32]P. M. Gehring, S.-E. Park, and G. Shirane, Phys. Rev. B **63**, 224109 (2001).
[33]P. M. Gehring, S. Wakimoto, Z.-G. Ye, and G. Shirane, Phys. Rev. Lett. **87**, 277601 (2001).
[34]D. La-Orauttapong, B. Noheda, Z.-G. Ye, P. M. Gehring, J. Toulouse, D. E. Cox, and G. Shirane, Phys. Rev. B **65**, 144101 (2002).
[35]S. Wakimoto, C. Stock, R. J. Birgeneau, Z.-G. Ye, W. Chen, W. J. L. Buyers, P. M. Gehring, and G. Shirane, Phys. Rev. B **65**, 172105 (2002).
[36]S. Wakimoto, C. Stock, Z.-G. Ye, W. Chen, P. M. Gehring, and G. Shirane, Phys. Rev. B **66**, 224102 (2002).
[37]J. Hlinka, S. Kamba, J. Petzelt, J. Kulda, C. A. Randall, and S. J. Zhang, Phys. Rev. Lett. **91**, 107602 (2003).
[38]C. Stock, R. J. Birgeneau, S. Wakimoto, J. S. Gardner, W. Chen, Z.-G. Ye, and G. Shirane, Phys. Rev. B **69**, 094104 (2004).
[39]C. Stock, D. Ellis, I. P. Swainson, G. Xu, H. Hiraka, Z. Zhong, H. Luo, X. Zhao, D. Viehland, R. J. Birgeneau, and G. Shirane, Phys. Rev. B **73**, 064107 (2006).
[40]P. M. Gehring, H. Hiraka, C. Stock, S.-H. Lee, W. Chen, Z.-G. Ye, S. B. Vakhrushev, and Z. Chowdhuri, Phys. Rev. B **79**, 224109 (2009).
[41]I. P. Swainson, C. Stock, P. M. Gehring, G. Xu, K. Hirota, Y. Qiu, H. Luo, X. Zhao, J.-F. Li, and D. Viehland, Phys. Rev. B **79**, 224301 (2009).
[42]A. Al-Zein, J. Hlinka, J. Rouquette, and B. Hehlen, Phys. Rev. Lett. **105**, 017601 (2010).
[43]W. Dmowski, S. B. Vakhrushev, I.-K. Jeong, M. P. Hehlen, F. Trouw, and T. Egami, Phys. Rev. Lett. **100**, 137602 (2008).
[44]B. Jaffe, W. R. Cook, and H. Jaffe, *Piezoelectric Ceramics* (Academic Press, New York, 1971).
[45]J. Hlinka, P. Ondrejkovic, M. Kempa, E. Borissenko, M. Krisch, X. Long, and Z.-G. Ye, Phys. Rev. B **83**, 140101 (2011).
[46]U. V. Waghmare and K. M. Rabe, Phys. Rev. B **55**, 6161 (1997).
[47]K. Oka, H. Unoki, H. Yamaguchi, and H. Takahashi, J. Cryst. Growth **166**, 380 (1996).
[48]R. A. Cowley, Phys. Rev. **134**, A981 (1964).
[49]M. J. Haun, E. Furman, S. J. Jang, H. A. McKinstry, and L. E. Cross, J. Appl. Phys. **62**, 3331 (1987).
[50]G. A. Rossetti and N. Maffei, J. Phys.: Condens. Matter **17**, 3953 (2005).
[51]M. D. Fontana, H. Idrissi, G. E. Kugel, and K. Wojcik, J. Phys.: Condens. Matter **3**, 8695 (1991).
[52]C. M. Foster, Z. Li, M. Grimsditch, S.-K. Chan, and D. J. Lam, Phys. Rev. B **48**, 10160 (1993).
[53]Z. Li, M. Grimsditch, C. Foster, and S.-K. Chan, J. Phys. Chem. Solids **57**, 1433 (1996).
[54]H. P. Soon, H. Taniguchi, Y. Fujii, M. Itoh, and M. Tachibana, Phys. Rev. B **78**, 172103 (2008).
[55]W. Zhong and D. Vanderbilt, Phys. Rev. Lett. **74**, 2587 (1995).
[56]G. Shirane, J. D. Axe, J. Harada, and A. Linz, Phys. Rev. B **2**, 3651 (1970).
[57]M. D. Fontana, G. Dolling, G. E. Kugel, and C. Carabatos, Phys. Rev. B **20**, 3850 (1979).
[58]R. Currat, R. Comes, B. Dorner, and E. Wiesendanger, J. Phys. C **7**, 2521 (1974).
[59]R. Currat, H. Buhay, C. H. Perry, and A. M. Quittet, Phys. Rev. B **40**, 10741 (1989).
[60]J. D. Axe, J. Harada, and G. Shirane, Phys. Rev. B **1**, 1227 (1970).
[61]R. Comès and G. Shirane, Phys. Rev. B **5**, 1886 (1972).
[62]C. H. Perry, R. Currat, H. Buhay, R. M. Migoni, W. G. Stirling, and J. D. Axe, Phys. Rev. B **39**, 8666 (1989).
[63]G. Shirane and Y. Yamada, Phys. Rev. **177**, 858 (1969).
[64]W. G. Stirling, J. Phys. C **5**, 2711 (1972).
[65]I. Tomeno, Y. Tsunoda, K. Oka, M. Matsuura, and M. Nishi, Phys. Rev. B **80**, 104101 (2009).
[66]P. Ghosez, X. Gonze, and J. P. Michenaud, Ferroelectrics **206**, 205 (1998).
[67]R. Yu and H. Krakauer, Phys. Rev. Lett. **74**, 4067 (1995).
[68]B. Jannot, C. Escribe-Filippini, and J. Bouillot, J. Phys. C **17**, 1329 (1984).
[69]E. Farhi, A. Tagantsev, R. Currat, B. Hehlen, E. Courtens, and L. Boatner, Eur. Phys. J. B **15**, 615 (2000).
[70]H. H. Barrett, Phys. Lett. A **26**, 217 (1968).
[71]W. Cochran and A. Zia, Phys. Status Solidi B **25**, 273 (1968).
[72]H. Fujishita and S. Hoshino, J. Phys. Soc. Jpn. **53**, 226 (1984).
[73]H. Fujishita and S. Katano, J. Phys. Soc. Jpn. **66**, 3484 (1997).
[74]A. Naberezhnov, S. Vakhrushev, B. Dorner, D. Strauch, and H. Moudden, Eur. Phys. J. B **11**, 13 (1999).
[75]S. G. Lushnikov, A. I. Fedoseev, S. N. Gvasaliya, and S. Kojima, Phys. Rev. B **77**, 104122 (2008).
[76]J.-H. Ko, D. H. Kim, and S. Kojima, Phys. Rev. B **77**, 104110 (2008).
[77]S. M. Farnsworth, E. H. Kisi, and M. A. Carpenter, Phys. Rev. B **84**, 174124 (2011).